# Shipboard determinations of the distribution of $^{13}$C in atmospheric methane in the Pacific

David C. Lowe, W. Allan, Martin R. Manning, Tony Bromley, Gordon Brailsford, Dominic Ferretti, Antony Gomez, Rob Knobben, Ross Martin, Zhu Mei, and Rowena Moss

National Institute of Water and Atmospheric Research, Wellington, New Zealand

K. Koshy and M. Maata

School of Pure and Applied Sciences, University of the South Pacific, Suva, Fiji

**Abstract.** Measurements of the mixing ratio and $\delta^{13}$C in methane ($\delta^{13}$CH$_4$) are reported from large, clean air samples collected every 2.5° to 5° of latitude on four voyages across the Pacific between New Zealand and the West Coast of the United States in 1996 and 1997. The data show that the interhemispheric gradient for $\delta^{13}$CH$_4$ was highly dependent on season and varied from $< 0.1‰$ in June 1996 to $> 0.5‰$ in November 1996 with an estimated annual mean of 0.2-0.3‰. The seasonal cycles in $\delta^{13}$CH$_4$ reveal three distinct latitude bands differentiated by phase. Maxima occur in January–February for the extratropical Southern Hemisphere, in September-October for the tropics, and in June-July for the extratropical Northern Hemisphere. The data are compared with results from a three-dimensional transport and atmospheric chemistry model that simulates the observed latitudinal structure of either $\delta^{13}$CH$_4$ or the methane mixing ratio well, but not both simultaneously. The requirement that a methane source-sink budget be consistent with both types of data clearly imposes stricter constraints than arise from either mixing ratio or isotopic data alone. The seasonal $\delta^{13}$CH$_4$ data in the extratropical Southern Hemisphere are used to estimate a value for the net fractionation in the CH$_4$ sink of 12-15‰, which is larger than can be explained by current laboratory measurements of a kinetic isotope effect for the OH + CH$_4$ reaction and soil sink processes. The hypothesis that the discrepancy is caused by competitive reaction of active chlorine with methane in the marine boundary layer is discussed.

## 1. Introduction

Determinations of methane in air trapped in bubbles in Antarctic ice show that the burden of atmospheric methane has more than doubled over the last 150 years [*Etheridge et al.*, 1992; 1998] owing to an excess of sources over sinks. Major sources of atmospheric methane include enteric fermentation in ruminant animals; methanogenesis in wetlands, rice paddies, and landfills; venting of natural gas, and emissions from biomass burning. About 90% of methane removal is believed to be due to oxidation in the troposphere by the hydroxyl radical (OH), with removal by soil bacteria and stratospheric losses considered to be of lesser importance [*Cicerone and Oremland*, 1988; *Tyler et al.*, 1990, 1994].

Extensive mixing ratio measurements made over several years at a number of sites in the Northern and Southern Hemispheres have been used to develop a consistent picture of the global methane budget using atmospheric chemistry and transport models [*Fung et al.*, 1991; *Dlugokencky et al.*, 1994; *Hein et al.*, 1997].

Measurements of variations in the isotopic composition of atmospheric methane have provided additional constraints on the budget because several of the sources can be distinguished by characteristic $^{14}$C, $^{13}$C, and $^{2}$D signatures [*Lowe et al.*, 1988; *Wahlen et al.*, 1989; *Tyler*, 1992; *Conny and Currie*, 1996; *Bergamaschi et al.*, 1998]. For example, methane produced by methanogenesis under anaerobic conditions is depleted in $^{13}$C [*Stevens and Engelkemeir*, 1988], whereas methane released from biomass burning is relatively enriched in $^{13}$C, retaining values close to that of the parent carbon in the fuel [*Bender*, 1971; *Hao and Ward*, 1993].

*Lowe et al.* [1991, 1994] and *Lassey et al.* [1993] have reported a series of $\delta^{13}$C measurements in atmospheric methane at Baring Head, New Zealand, 41°S, and Scott Base, Antarctica, 78°S, which show irregular seasonal cycles and no latitudinal gradient in the extratropical Southern Hemisphere. They suggest that these cycles are driven by the southward transport of isotopically enriched methane derived from tropical biomass burning.

In this work we describe new high-precision determinations of $\delta^{13}$C in atmospheric methane derived from the tropical Pacific from a shipboard air-sampling program. The aims of the program include determination of the interhemispheric gradient of $\delta^{13}$C in atmospheric methane, its seasonal variations, identification of tropical biomass burning sources of methane, and better understanding of methane transport into the

extratropical Southern Hemisphere. The first data from the programme are reported here together with their interpretation and comparison with a three-dimensional (3-D) transport and chemistry model.

## 2. Experimental

### 2.1. Air Sample Collection Techniques

Our program uses the Blue Star Line (now part of P&O Nedlloyd) container ships, the *Melbourne Star* and the *Argentina Star*, which make frequent voyages between New Zealand and the West Coast of the United States. The container ships are used as a platform to collect large, clean, dry whole air samples representative of the Pacific, on great circle routes between Auckland (New Zealand), Suva (Fiji), Honolulu (Hawaii), Los Angeles, and Seattle (U.S. West Coast). A typical voyage track (*Melbourne Star* in June 1996) is shown in Fig. 1.

Depending on wind direction, the air is sampled through either port or starboard Dekabon type 1300 (Furon Dekoron, Aurora, Ohio) 12.7 mm OD air lines, respectively 35 and 50 m long, mounted on either side of the ship's bridge with the inlet well forward of the engine exhaust funnels. Air is filtered and dried by passage through stainless steel traps, 30 cm long and 8 cm in diameter, containing ~200 g of 3 mm pellets of 13X molecular sieve (Alltech, Deerfield, Illinois). The molecular sieve drying traps are regenerated before each sampling by reverse flushing with dry air at 50 mL min$^{-1}$ at 280°C for at least 8 hours and 10 hours after sampling humid tropical air.

Large air samples, approximately 1 m$^3$ (STP) each, are collected using a specially modified high-purity RIX Industries (Oakland, California) clean air diving compressor type SA-3 [*Mak and Brenninkmeijer*, 1994]. The samples are stored in high-pressure "Aculife" treated (Scott Specialty Gases, San Bernadino, California) aluminium cylinders. The compressor and storage cylinders are located behind and one deck below the ship's bridge. Before a sample is collected, the cylinders are flushed three times to a pressure of 7 bar with sample air and vented before the final sample is collected at a pressure of ~50 bar. Samples are collected every 5° of latitude and more frequently as the ship passes through the Intertropical Convergence Zone (ITCZ), typically every 2.5° of latitude. Wind fields from the European Centre for Medium-Range Weather Forecasts (ECMWF), satellite cloud pictures, and meteorological observations during the voyage are used to track the position of convergence zones in the Pacific.

The large air samples in the cylinders are complemented by air samples collected in 2 L glass flasks using a separate, low pressure, 1.5 bar, clean air Thomas (Sheboygan, Wisconsin) diaphragm pumping system. These samples are collected in pairs and used as controls for the large cylinders. The glass flasks have a dip tube and dual Glass Expansion (Melbourne, Australia) piston valves fitted with Teflon "O" rings. These flasks are preevacuated and flushed with sample air 5 times prior to collection, and the sample is collected through a 2 m long, 6.4 mm OD Dekabon 1300 line adjacent to the compressor air intakes. After the voyage, the air samples are returned to the National Institute of Water and Atmospheric Research (NIWA) laboratory in Wellington, New Zealand, where the large air samples are measured for mixing ratio, $^{13}C/^{12}C$ and $^{14}C/^{12}C$ of atmospheric CH$_4$ and CO. The flask samples are measured for mixing ratios of CH$_4$, CO, N$_2$O, and C$_2$-C$_6$ nonmethane
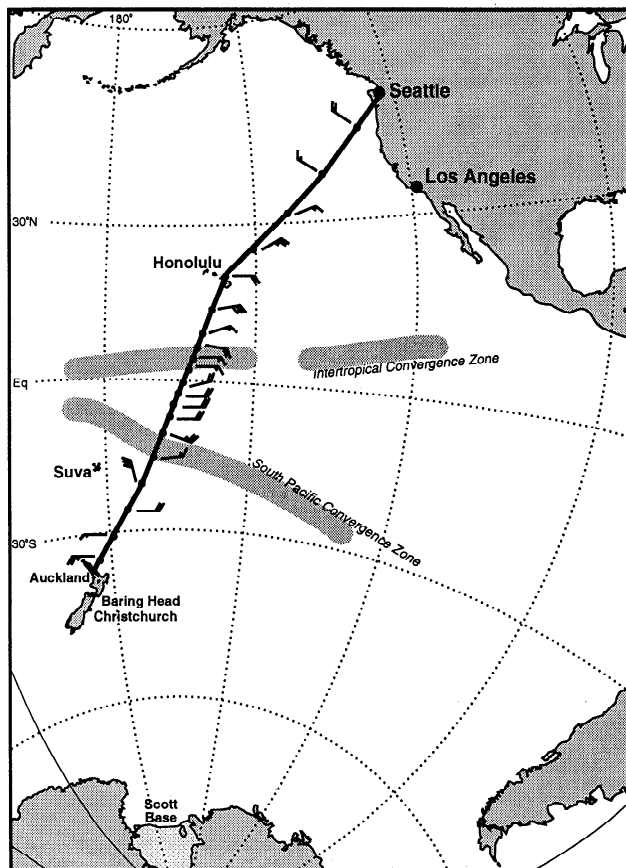


**Figure 1.** The Pacific voyage route taken by the container ship, *Melbourne Star* in June 1996 between Auckland and Seattle. Positions of the Intertropical Convergence Zone (ITCZ) and South Pacific Convergence Zone (SPCZ) and wind speed and direction at the sampling sites for the large air samples are, shown. For clarity the routes for the other voyages referred to in the text are omitted.

hydrocarbons. These results test the integrity of the large air samples providing a check for possible contamination introduced by either the compressor pumping system or shipboard sources. A subset of the flasks is also sent to the U.S. National Oceanic and Atmospheric Administration Climate Monitoring and Diagnostics Laboratory (NOAA CMDL) in Boulder, Colorado, for analyses of CH$_4$, CO, CO$_2$, and N$_2$O mixing ratios as an intercomparison with the NIWA determinations. This work considers only measurements of methane, and results for other species will be reported separately.

### 2.2. Gas Chromatography

Mixing ratio determinations of the trace gases in the 2 L flasks and aluminium cylinders are made using gas chromatography. The air in the flasks is dried before analysis, and all results are reported as mixing ratios, ppb (nmol mol$^{-1}$), in dry air. The CH$_4$ measurements are made using a Hewlett Packard HP5890 series II gas chromatograph (GC) fitted with a flame ionization detector (FID). The chromatography is performed on a 180 cm long, 3 mm diameter, packed 5A molecular sieve analytical column (Alltech, Deerfield, Illinois). This is preceded by an identical 40 cm long precolumn. A 10-

port Valco (Houston, Texas) injection valve is used to backflush this during each sample injection to prevent carbon dioxide, water, and nonmethane hydrocarbons from reaching the main analytical column. Each sample is measured 5 times between alternate working standard injections, and the precision of the measurement (1 $\sigma$) is typically better than 2 ppb. The methane concentrations are reported with respect to primary standard reference materials (SRMs) prepared by the U.S. National Institute of Standards and Technology (NIST), and the laboratory working standards are calibrated against these. In the literature, another scale has been widely reported by NOAA CMDL [Lang et al., 1990; 1992], and our estimate of the ratio of the NOAA CMDL scale to the NIST values is 0.986. CO mixing ratio measurements are made using a reduction gas detector by Trace Analytical Ltd. (Menlo Park, California), and light NMHC, $C_2$-$C_6$, are determined using the techniques of Greenberg et al. [1994].

## 2.3. Air Sample Methane to $CO_2$ Conversion for IRMS

To determine $^{13}C/^{12}C$ ratios in methane from the large air samples, we use a gas source isotope ratio mass spectrometer (IRMS). However, the methane must first be quantitatively extracted from the air samples and converted to $CO_2$. This is done on a vacuum conversion line using a modification of a "flow through" procedure developed by Lowe et al. [1991] and inspired by the early work of Stevens and Krout [1972]. First, the air sample is stripped of remaining water, $CO_2$, $N_2O$, and NMHC by passage at 1 L min$^{-1}$ (controlled by an integrating mass flow controller) through a series of cryogenic traps held at liquid nitrogen temperature. In addition, CO is removed from the stream by passage through a 350 g bed of Schütze reagent (Leco Corporation, St. Joseph, Missouri), where the active reagent is iodine pentoxide on a silica gel support. Subsequently, methane in the air sample is combusted at 790°C in a furnace containing 100 g of 1% platinum catalyst supported on 3 mm alumina pellets (Aldrich, Milwaukee, Wisconsin). The resulting $CO_2$, which retains the $^{13}C/^{12}C$ and $^{14}C/^{12}C$ ratios from the methane in the air samples, and water from the combustion are collected in cryogenic traps immediately after the furnace. The water is removed at -80°C in alcohol dry ice traps by triple vacuum distilling the $CO_2$ from the cryogenic traps into small pyrex bottles or flame-sealed pyrex tubes. This $CO_2$ is analyzed for $^{13}C$ by IRMS, and the same gas may be used for $^{14}C$ determinations by conversion into graphite targets for accelerator mass spectrometry [Lowe et al., 1991].

Conversion yields for the process are calculated using the collected $CO_2$ pressure and volume in a calibrated manometer at room temperature compared with the $CO_2$ expected on the basis of the air sample methane mixing ratio and the amount of air processed as determined by an integrating mass flow controller. Measured yields are ~100% and subject to errors of ~2% in each of the manometer pressure times volume determinations and measurement errors in the integrating mass flow controller.

## 2.4. Stable Isotope Ratio Mass Spectrometry

The $^{13}C/^{12}C$ ratio measurements of the $CO_2$ derived from the methane are made at NIWA using a Finnigan MAT (Bremen, Germany) 252 IRMS running in dual-inlet mode. The sample inlet side of the IRMS has been modified by inserting a 500 μL cold finger stainless steel volume at the head of the sample capillary with the inlet isolated by a pneumatically actuated, gold-seated dual valve (Finnigan MAT, Bremen). This allows the direct introduction of 10-80 μL $CO_2$ samples from volumes

of either 0.5 or 2.5 mL into the IRMS ion source. With this inlet system, $m/z = 44$ signals are typically 4 V (collector resistance 3 x $10^8$ $\Omega$) for the container ship atmospheric methane samples and the precision of individual $\delta^{13}C$ determinations (10 changeovers between sample and working reference) is typically 0.01‰.

We use the standard notation

$$\delta^{13}C = (R_s/R_r - 1) \times 1000 \ (‰) \qquad (1)$$

to calculate $^{13}C/^{12}C$ ratios as parts per mill (‰) where $R_s$ and $R_r$ are the $^{13}C/^{12}C$ ratios of the unknown sample and a working reference gas, respectively. The working reference is dry $CO_2$ stored in a 25 L glass flask at 1.1 bar and is metered as required via 3 mm OD stainless steel lines and Nupro (Nupro, Willougby, Ohio) high-vacuum valves into the variable volume bellows on the reference side of the MAT 252. The reference $CO_2$ was made from combusted, purified, landfill methane and mixed with $CO_2$ derived from marine carbonates to produce a $\delta^{13}C \approx -47‰$, which is in the middle of the range expected for atmospheric methane samples. Two working references, denoted CH4WR1 and CH4WR2, were prepared in this fashion. These isotopically "light" $CO_2$ working reference gases are compared with $CO_2$ evolved every 6-12 months from NBS19 carbonate supplied by the International Atomic Energy Agency (IAEA), Vienna, Austria [Gonfiantini et al., 1993]. This provides the link to the (V-PDB) scale widely used in the literature and all measurements reported here are as per mill deviations from V-PDB. CH4WR1 and CH4WR2 were first determined at $\delta^{13}CH_4$ = -47.07 ± 0.01 and -47.02 ± 0.01‰ V-PDB, respectively, versus NBS19 in January 1995, and repeated comparisons since then show that any drift in these values is less than 0.005‰ in 3 years. In this work, we will refer to the $\delta^{13}C$ of the carbon in methane as "$\delta^{13}CH_4$," noting that this is for ease of nomenclature only.

An additional assurance of calibration is provided by a light barium carbonate reference material supplied by the IAEA in Vienna, IAEA-CO-9, also known as NZCH [Gonfiantini et al., 1993; Lowe et al., 1991]. The published values for this material are $\delta^{13}C$ = -47.119 ± 0.149‰ and $\delta^{18}O$ = -15.282 ± 0.093‰. $CO_2$ from this material is evolved and compared with NBS19 and the working references, CH4WR1 and CH4WR2, as described above. Quality assurance is also provided by the routine measurement of $\delta^{13}CH_4$ in methane mixtures in synthetic air and ambient methane in dry air samples collected at Baring Head, New Zealand, and stored or "archived" in stainless steel tanks as described by Lowe et al. [1994]. These controls provide confidence in the sample preparation and analysis techniques and the $\delta^{13}CH_4$ data reported here. The overall precision of the technique, 1 $\sigma$, as determined by $\delta^{13}CH_4$ analyses of sets of duplicate air samples collected at Baring Head, is 0.02‰. Intercalibration has also routinely been carried out with other laboratories making $\delta^{13}CH_4$ measurements in air. For example, a set of 15 air samples exchanged between Paul Quay, University of Washington, Seattle, and NIWA and analyzed for $\delta^{13}CH_4$ by both laboratories showed a mean difference of 0.01±0.05‰ [Lowe et al., 1994]. A similar intercalibration exercise is currently in progress with the Geosciences Department, University of California, Irvine, and a set of 16 samples exchanged between the two laboratories from early 1995 to mid-1998 shows a mean analysis difference for $\delta^{13}CH_4$ of 0.01±0.06‰.
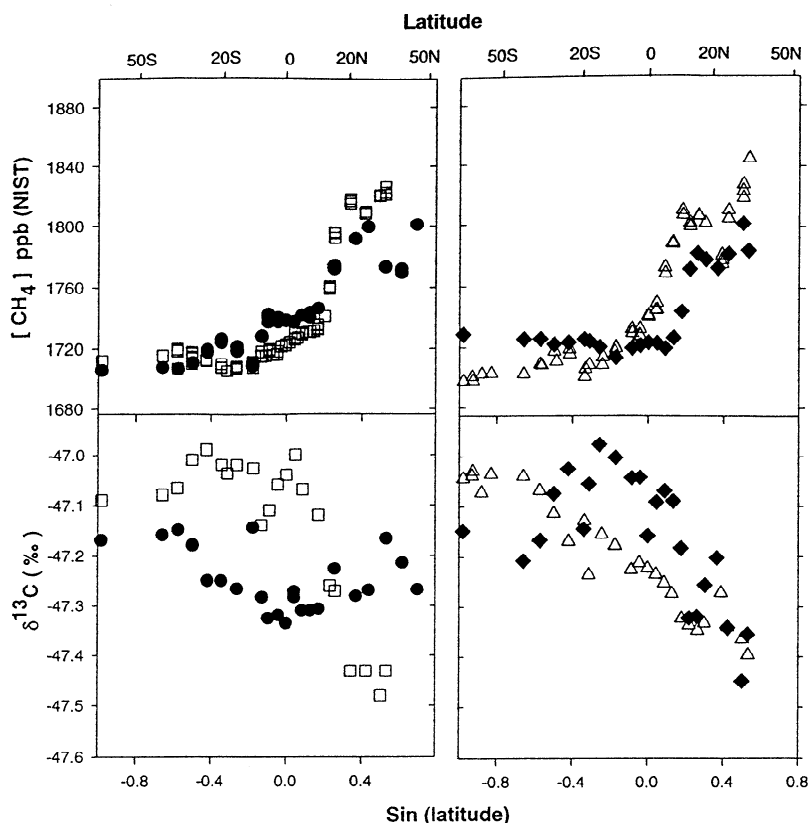
**Figure 2.** (top) Methane mixing ratio and (bottom) $\delta^{13}CH_4$ data from Pacific container ship voyages, Suva (17°S), Baring Head (41°S), Scott Base (78°S), and a tropospheric flight between Christchurch (43°S) and McMurdo Sound (78°S). (left) Data from June 1996 (solid circles) and November 1996 (open squares). (right) Data from February 1997 (open triangles) (includes the Antarctic tropospheric flight) and September 1997 (solid diamonds). For clarity, data from the surface sites and the flight are not shown as separate symbols, but they can be located by referring to their latitudes. Typical analytical errors for the mixing ratio and $\delta^{13}CH_4$ determinations are detailed in the text and symbols are omitted here.

## 3. Discussion

### 3.1. Results

Methane mixing ratio measurements for air samples collected on the four container ship voyages are plotted as a function of sine of latitude in Figure 2. The voyages took place in June and November 1996 (*Melbourne Star*) and February and September 1997 (*Argentina Star*). Time coincident data from Suva, Fiji, 17°S; Baring Head, New Zealand, 41°S; Scott Base, Antarctica, 78°S; and data from a C130 flight in the troposphere between Christchurch, New Zealand, 43°S; and McMurdo Sound, Antarctica, 78°S, in February 1997 are also plotted in Figure 2. The flight samples, five in total, were collected at altitudes ranging from 3.9 to 5.0 km, well within the troposphere, using techniques described by *Lowe et al.* [1991]. All data sets show relatively uniform mixing ratios between 78° and ~30°S, indicative of a well-mixed extratropical Southern Hemisphere. However, north of 15°S, a typical position for the South Pacific Convergence Zone (SPCZ) at 170°W [*Trenberth*, 1991] (see Figure 1), mixing ratio data from the voyages showed quite different trends. For example, the voyages in November 1996 and February 1997 showed a steady increase from ~1710 to 1740 ppb between 10°S and 10°N, the position of the ITCZ. Here there was an abrupt transition to much higher and more variable values ranging from 1740 to 1840 ppb, indicative of the

extratropical Northern Hemisphere. Higher methane mixing ratios are expected north of the ITCZ, because most methane sources are in the Northern Hemisphere. For the June 1996 voyage, however, a local minimum of 1710 ppb occurred at the position of the SPCZ, 10°S, followed by a rapid rise to 1740 ppb by 5°S. Thereafter the mixing ratio was fairly uniform up to the ITCZ located at ~10°N. Thus on the voyage route in June 1996, a well-defined SPCZ and ITCZ led to a confined region of well-mixed air in the equatorial Pacific showing methane mixing ratios midway between the extratropical Southern and Northern Hemispheres. In September 1997 the meteorological situation was quite different, with no significant SPCZ present but a well-defined ITCZ at 12°N, and the methane mixing ratio data were relatively uniform from 78°S to the ITCZ. Seasonal differences in mixing ratio gradients on the voyages were observed with the largest, ~110 ppb, occurring in February 1997 and the smallest, ~60 ppb, in September 1997 (Figure 2). These correlate well with the difference in the phases of the mixing ratio cycles in each hemisphere. *Vincent* [1994] reports that the position and intensity of the SPCZ vary seasonally and that it is generally more active in the southern summer. The limited data set presented here suggests that the strength and position of the SPCZ are important factors in the transport of methane into the extratropical Southern Hemisphere from tropical regions and the Northern Hemisphere. Knowledge of the position, extent, and strength of the convergence zones is clearly essential in
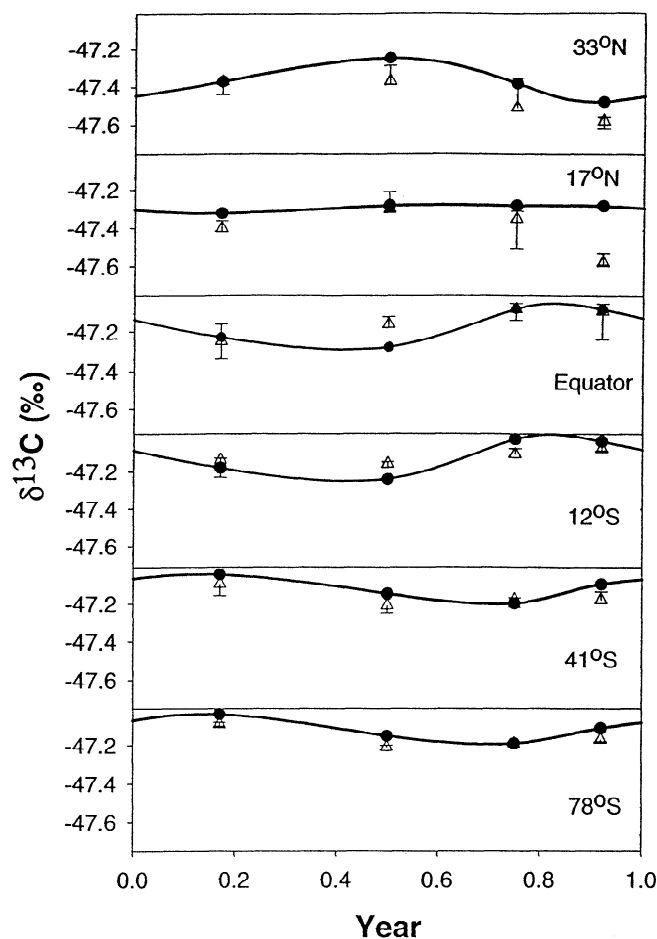
**Figure 3.** Mid-Pacific latitudinal cycles in $\delta^{13}CH_4$. The solid lines and dots in the 33°N, 17°N, equator, and 12°S panels show data interpolated as a complete seasonal cycle from the four container ship voyages using a harmonic fit for these latitudes. The solid lines and points in the 41°S and 78°S panels show concurrent data from Baring Head and Scott Base, also fitted with a harmonic fit. The open triangles are seasonal predictions for the same latitudes made by the 3-D chemical tracer model, TM2, as described in the text. The positive and negative "error bars" on the triangles show the maximum and minimum $\delta^{13}CH_4$ obtained when the model is run within 10 days on either side of the ship measurement day.

interpreting atmospheric trace gas data obtained on trans-Pacific voyages.

The $\delta^{13}CH_4$ data for the four container ship voyages are also shown in Figure 2 with equivalent data from the other sites and the aircraft flight described above. In the June 1996 voyage from Auckland to Seattle, we measured a relatively uniform decrease in $\delta^{13}C$ from –47.15‰ at 35°S to a minimum value of –47.35‰ at the equator. However, there was a sharp increase in $\delta^{13}CH_4$ to –47.15‰ at 10°S, which anticorrelated with a minimum in methane concentration and coincided with the position of the SPCZ. In the Northern Hemisphere, $\delta^{13}CH_4$ increased gradually to ~ –47.30‰ at 20°N. No abrupt change was observed at the ITCZ, located at ~10°N, and the observed average gradient from the data reported here in $\delta^{13}CH_4$ between the hemispheres is relatively small, less than 0.1‰. In November 1996, however, a large gradient between the hemispheres was measured in $\delta^{13}CH_4$, with relatively small variations ranging from ~ –47.00

to –47.10‰ up to about 5°N, followed by a rapid drop to ~ –47.50‰ at ~30°N. In February 1997, $\delta^{13}CH_4$ showed a virtually monotonic decrease from ~ –47.05‰ at 78°S to –47.35‰ at 30°N, with most values falling midway between the June and November 1996 data. The September 1997 voyage, however, featured a broad but pronounced maximum in $\delta^{13}CH_4$ at ~10°S with minimum values in the midlatitudes of both hemispheres.

The $\delta^{13}CH_4$ data shown in Figure 2 exhibit marked seasonal behavior with cycles quite unlike those observed for the concurrent methane mixing ratio data or similar shipboard atmospheric methane mixing ratio data reported for the Pacific by *Dlugokencky et al.* [1994]. In Fig. 3 we plot average seasonal cycles in $\delta^{13}CH_4$ for Baring Head and Scott Base from data reported by *Lowe et al.* [1997]. In addition, seasonal cycles in $\delta^{13}CH_4$ are interpolated from the data obtained from the four voyages and plotted as a single year at the latitudes 33°N, 17°N, the equator, and 12°S. All six data sets are fitted with harmonic functions (constant plus 12 month period) and show three distinct cycle types differentiated by the phase of the maxima and minima. In the extratropical Southern Hemisphere at both Baring Head and Scott Base, there is a pronounced seasonal cycle with a maximum in January-February and a minimum in August-September. In the tropics, however, the phase of the observed seasonal cycle is shifted by 2 months, with a maximum in October and a minimum in June. Inspection of Figure 2 shows that $\delta^{13}CH_4$ data from all four voyages are virtually identical at 17°N, and hence there is no significant seasonal cycle shown at this latitude in Figure 3. At 33°N the seasonal cycle is almost 6 months out of phase with those seen in the tropics. Farther north at Olympic Peninsula, 48°N, on the Washington coast, and Barrow, Alaska, 72°N, *Quay et al.* [1991] report irregular seasonal cycles in $\delta^{13}CH_4$ with phases similar to those observed at 33°N. *Tyler et al.* [1999a] report seasonal cycles in $\delta^{13}CH_4$ at Montano del Oro on the California coast, 35°N, and Niwot Ridge, Colorado, 41°N, with maxima in June, minima in November, and a peak-to-peak amplitude of 0.2-0.3‰.

Examination of Figure 3 shows that the maximum of the cycle at 33°N in June is ~ –47.25‰, which is similar in magnitude to the seasonal minimum observed at Baring Head and Scott Base. Since the tropical data show a minimum of ~ –47.30‰ at this time, no significant interhemispheric gradient in $\delta^{13}CH_4$ data on the voyage in June 1996 was observed. For the November 1996 voyage, however, the situation was quite different, with the minimum of seasonal cycles in the northern Pacific coinciding with maximum values in the Southern Hemisphere. This, coupled with the fact that, on average, $\delta^{13}CH_4$ is lower in the Northern than the Southern Hemisphere, led to a relatively large interhemispheric gradient of 0.5‰. Hence simple interpolation between the minimum and maximum gradients observed suggests that, to a first-order approximation, the annual average interhemispheric gradient in $\delta^{13}CH_4$ in the Pacific region covering 48°N to 35°S is ~0.2-0.3‰. However, this approximation is probably true for the entire Pacific region to the poles, because *Lowe et al.* [1991] show that there is no significant gradient in $^{13}CH_4$ from New Zealand south to the South Pole. Also, runs of the three-dimensional transport and atmospheric chemistry model TM2 (see section 3.4) suggest that there is no significant gradient (<0.05‰) between 48°N and 75°N. In addition, data published by *Quay et al.* [1991] show that there was no significant gradient (<0.05‰) in $^{13}CH_4$ between Olympic Peninsula, Washington (48°N), and Point Barrow, Alaska (71°N), during the years 1987 to 1989.

## 3.2. Kinetic Isotope Effect

The principal removal mechanism for methane from the atmosphere is believed to be chemical destruction by the OH radical, and hence, because $^{12}CH_4$ reacts faster with OH than $^{13}CH_4$, methane remaining in the atmosphere becomes enriched in $^{13}C$ relative to the global source. This process has been investigated under laboratory conditions, and a kinetic isotope effect (KIE) defined as the ratio of the rate constants of the reaction of OH with $^{12}CH_4$ and with $^{13}CH_4$ has been measured at 1.0054, or 5.4‰, by *Cantrell et al.* [1990] and recently by *Saueressig et al.* [1999] at 3.9‰ at 296 K. Consequently, as methane "ages" after emission to the atmosphere, the methane remaining in the atmosphere becomes progressively enriched in $^{13}C$ as it is oxidized by OH. A simple two-box model, one for each hemisphere, with sources in the Northern Hemisphere only, an interhemispheric exchange time of 1 year, and a KIE for CH₄ + OH of 1.005 (5‰) leads to a steady state interhemispheric gradient in $^{13}CH_4$ of 0.5‰, with the Southern Hemisphere more enriched. In the steady state situation, methane flows in both directions across the ITCZ. When typical methane sources, for example, from *Hein et al.* [1997], are included in the model for both hemispheres, the calculated average gradient reduces to 0.24‰, consistent with the average interhemispheric gradient, 0.2-0.3‰, deduced from the data in shown in Figure 2.

Seasonal changes in OH lead to seasonal changes in the destruction rate of methane in the atmosphere and consequent increases in $\delta^{13}CH_4$ as methane is removed from the atmosphere. As shown by *Lowe et al.* [1994], to a first approximation in the extratropical Southern Hemisphere, seasonal cycles in $\delta^{13}CH_4$ and methane mixing ratio can be used to estimate the "apparent" KIE of the methane removal process. Using the same approach, the data in Figure 2 suggest an "apparent" KIE in the range of 12-15‰. This is much larger than the laboratory values reported by *Cantrell et al.* [1990] and *Saueressig et al.* [1999]. The discrepancy could be explained by competitive removal of methane by other chemistry, for example, by active chlorine as suggested by *Gupta et al.* [1996]. *Saueressig et al.* [1995] and *Tyler et al.* [1998] have reported a relatively large KIE for the Cl + CH₄ reaction of 66‰ at 297 K and 66‰ at 299 K, respectively. Rate constants for the reaction at this temperature are a factor of ~15 larger for methane removal by chlorine than OH [*DeMore et al.*, 1997]. Using these data in a simple, weighted mean calculation shows that the active chlorine required, in conjunction with OH, to produce an apparent KIE of 12-15‰ would be ~$10^4$ atoms .cm$^{-3}$. Current estimates of mean levels of active chlorine in the marine boundary layer of ~$10^3$ cm$^{-3}$ [*Singh et al.*, 1996; *Graedel and Keene*, 1995] appear to be too low to account for the apparent KIE inferred from the data reported here. However, recent modeling studies by *Vogt et al.* [1996] and *Sander and Crutzen* [1996] suggest halogen activation routes which can lead to much higher chlorine atom concentrations. For example, *Vogt et al.* [1996] show that, if recycling reactions on sulfate aerosol are included, Cl-atom concentrations can reach $10^4$ atoms .cm$^{-3}$ at steady state. In addition, they find that sea-salt aerosol content is a critical parameter and that, if this increased by a factor of 5 to ~50 μg NaCl. m$^{-3}$ of air (the upper range of values typically found in the marine boundary layer(MBL)), reactive chlorine concentrations increase to 3-5 $10^4$ atoms .cm$^{-3}$. Thus the data reported here raise the interesting possibility that $^{13}CH_4$ may provide an independent technique for estimating alternative mechanisms for methane destruction and levels of species like active chlorine in the remote MBL.

## 3.3. The $\delta^{13}CH_4$ From Biomass Burning

Large-scale biomass burning occurs in the tropics and subtropics, particularly the southern tropics during the dry period of August to October [*Fishman et al.*, 1991; *Hao and Ward*, 1993; *Hao and Liu*, 1994]. These regions contain tropical rain forests comprising C3 plants with $\delta^{13}C$ about –28‰, and Savannah regions with C4 plants, $\delta^{13}C$ about –13‰ [*Bender*, 1971]. Methane produced during biomass burning is known to have a $\delta^{13}C$ value near that of the carbon in the parent material [*Stevens and Engelkemeir*, 1988] and is therefore considerably more enriched in $^{13}C$ than atmospheric methane. The $\delta^{13}CH_4$ data from the voyage of September 1997 show a large, broad peak in the southern tropics, with a maximum at ~12°S, consistent with the release of methane enriched in $^{13}C$ from biomass burning in the dry season in the Southern Hemisphere. The data were coincident with large fires, and widespread areas of smoke reported from Kalimantan to Sumatra caused by an intense El Niño induced drought in the latter part of 1997 [*Swinbanks*, 1997] and similar to the situation caused in the El Niño-Southern Oscillation event of 1991 [*Salafsky*, 1994]. Also, as shown in the following section, the presence of a tropical biomass burning source of methane leads to the prediction of relatively steep interhemispheric gradients in $\delta^{13}CH_4$, consistent with the observations in September 1997 and November 1996. In addition, concurrent CO mixing ratio data from the voyage show values consistently above those predicted by TM2 model runs (P. Bergamaschi, unpublished data, 1999) indicating the distribution of CO from various sources including methane from biomass burning. Work on the CO mixing ratio and isotope data and measurements of other species obtained from the container ship voyages is in progress and will be reported elsewhere.

## 3.4. Modeling

We compare the data presented here with results from a three-dimensional transport and atmospheric chemistry model TM2, developed at the Max-Planck-Institut für Meteorologie in Hamburg, Germany [*Heimann*, 1995; *Hein et al.*, 1997]. The model solves the continuity equation for atmospheric tracers on an Eulerian grid spanning the entire globe. In the present case, stored meteorological fields based on the 12-hourly meteorological analyses for 1987 from the European Centre for Medium-Range Weather Forecasts (ECMWF) in Reading, England, drive the transport. We expect that the use of stored meteorological fields for 1987 will be adequate for predicting the general features of methane spatial and temporal structure in 1996-1997. This opinion is based on the TransCom 2 comparison of model results for the long-lived SF₆ tracer by *Denning et al.* [1999] who state, "The differences among models are best explained in terms of differences in the intensity of subgrid-scale parameterized vertical transport rather than in terms of distinctions between CTMs and GCMs, or the use of analyzed wind observations rather than GCM simulated winds for the resolved transport."

We employ the "coarse grid" version of the model, which uses a horizontal grid of ~8° latitude by 10° longitude and a σ coordinate system with nine layers in the vertical direction. The model calculates the source and sink processes affecting each tracer, followed by calculation of the transport processes, at intervals of 4 hours. Eleven different source types are used with geographic and temporal variation as used by *Fung et al.* [1991]. Soil absorption is included as a negative source of strength –30 Tg yr$^{-1}$, as discussed by *Fung et al.* [1991]. Methane is

**Table 1.** Methane Source Budget Modified From *Francey et al.* [1999] and Lassey et al. Submitted manuscript, 1998, based on Intergovernmental Panel on Climate Change source strengths [*Prather et al.*, 1995; *Schimel et al.*, 1996].

| Source Type | Strength, Tg $CH_4$ yr$^{-1}$ | $\delta^{13}CH_4$, ‰ |
|---|---|---|
| Animals | 125 | −63 |
| Wetlands | | |
|   Bogs/tundra | 45 | −64 |
|   Swamps/alluvial | 95 | −59 |
| Rice | 65 | −62 |
| Landfills | 65 | −51 |
| Natural gas vents | 20 | −40 |
| Natural gas leaks | 65 | −40 |
| Coal mining | 45 | −38 |
| Biomass burning | 45 | −25 |
| Termites | 20 | −62 |
| Total | 590 | −52.85 |
| Soil absorption | −30 | −69 |
| Total | 560 | −51.98 |

The soil absorption sink is given as a negative source. The chosen $\delta^{13}CH_4$ is discussed in the text. The $\delta^{13}CH_4$ values are based on *Hein et al.* [1997], *Francey et al.* [1999], and *Lassey et al.* [1999].

\* Values denote the weighted mean.

destroyed mainly by tropospheric OH, and we follow *Fung et al.* [1991] in using the OH number density fields calculated by *Spivakovsky et al.* [1990]. These are scaled by a single numerical multiplying factor to produce OH number density fields that, when included in a model run, give an atmospheric $CH_4$ + OH lifetime of ~9 years as suggested by *Schimel et al.* [1996]. The source strengths used are adapted from those derived from recent budget analyses [*Francey et al.*, 1999; *Prather et al.*, 1995; *Lassey et al.*] and are shown in Table 1. A total source strength of 590 Tg yr$^{-1}$ is employed, consistent with recent Intergovernmental Panel on Climate Change (IPCC) assessments [*Schimel et al.*, 1996].

The soil sink for methane is taken to have a fractionation of −22‰ [*Tyler et al.*, 1994]. This means that the methane oxidized is ~22‰ more depleted in $^{13}C$ than the atmospheric methane from which it is drawn. Thus, for a typical atmospheric methane $\delta^{13}C$ of −47‰, the methane flow to the sink would have a $\delta^{13}C$ value of ~ −69‰. In Table 1, we treat the soil sink as if it were a negative source of −30 Tg yr$^{-1}$. The sink fractionation of −22‰ has undetermined seasonality and is accurate only to ~ ±4‰ [*Tyler et al.*, 1994]. This exceeds the variation of $\delta^{13}C$ in atmospheric methane, so we adopt the $\delta^{13}C$ value −69‰ in Table 1 for the effective negative source at all locations and seasons.

Note that there is not a one-to-one correspondence between our source structures and those used by *Spivakosky et al.* [1990]. However, recent modeling studies have made it clear that fine details of the OH distribution used do not significantly affect the modeled structure of long-lived atmospheric species. For example, *Houweling et al.* [1998] used two very different OH fields to determine the distribution of methyl chloroform (a species with a similar lifetime to methane) and found very small differences in the modeled structure of the methyl chloroform

(see their Figure 10). We therefore do not consider that the differences between OH fields derived from a full interactive calculation and those used in our approach would make a significant difference to methane gradients and distributions in our model results.

Each methane source is run separately and normalized to 1 Tg $CH_4$ yr$^{-1}$, giving a "building block" of equilibrium mixing ratios determined from the final year of a 50-year run. These building blocks are then combined in a weighted sum using the source strengths in Table 1 to give the global methane mixing ratio field. Another set of building blocks for $^{13}CH_4$ is obtained by running the model for 50 years with the decay rate field multiplied by 1/1.0054 to represent a KIE of 5.4‰. The $^{13}CH_4$ building blocks are then combined in another weighted sum using the source $\delta^{13}C$ values in Table 1 to give the global $^{13}CH_4$ field and hence a $\delta^{13}CH_4$ field. The model will be described in more detail elsewhere.

The source strength and $\delta^{13}C$ values in Table 1 are chosen within the ranges reported in the literature [e.g., *Hein et al.*, 1997] to give yearly mean mixing ratio and $\delta^{13}CH_4$ values comparable with those observed at Baring Head after the equilibrium model results have been adjusted by −45 ppb and −0.38‰. These adjustments are derived from Figure 3 of *Lassey et al.*, [1999], which shows the evolving extent of disequilibrium in a simple global model.

Overall, the TM2 results for the budget in Table 1 predict a difference in the annual mean $\delta^{13}CH_4$ between 41°S latitude and 33°N latitude of 0.27‰, consistent with the experimental value of 0.2 − 0.3‰ discussed in section 3.1. However, the simulated annual mean mixing ratio gradient between these latitudes is significantly larger than that observed. Model results sampled along the ship transits through the TM2 space/time fields are shown in Figure 4 in the same format as the observations in
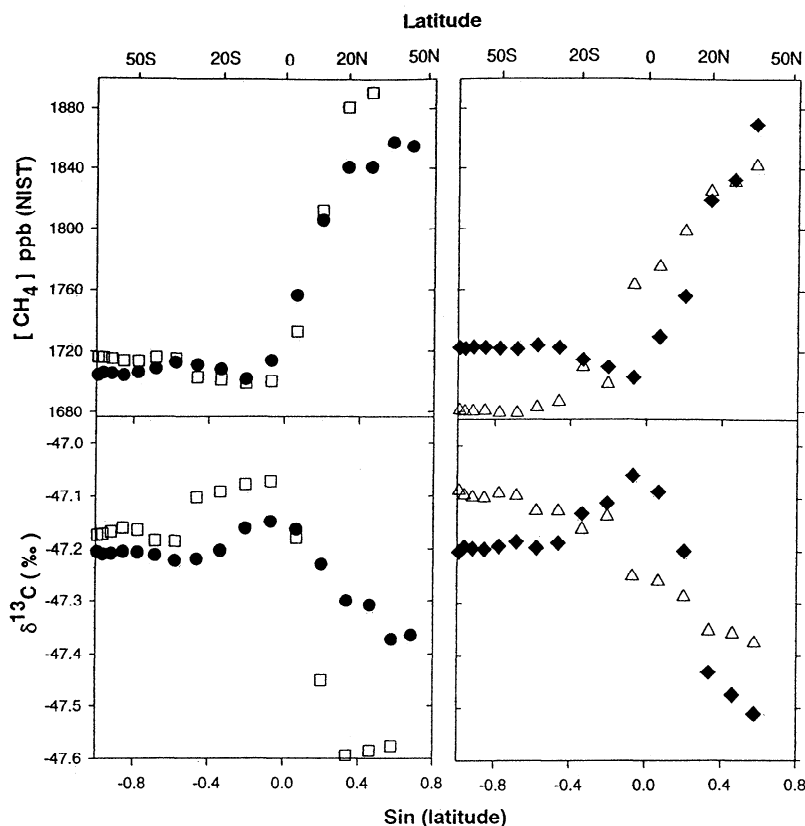
**Figure 4.** Simulated data for ship transits from the TM2 output fields for positions and times corresponding to the observations shown in Figure 2. The symbols for the months of February, June, September, and November correspond to those described in Figure 2.

Figure 2. The mixing ratio latitudinal structures in Figure 4 (top) are qualitatively similar to those in Figure 3, but the magnitudes of the gradients are typically of the order of 40% larger, except for the February transit, in which the gradient is only about 6% larger.

The latitudinal structures of $\delta^{13}CH_4$ shown in Figure 4 (bottom) are both qualitatively and quantitatively quite similar to the observations in Figure 2. Particularly noteworthy are the steep gradients in $\delta^{13}CH_4$ just northward of the equator in September 1997 and November 1996, which are missing in February 1997 and June 1996. A model run with the biomass burning source omitted confirmed that these steep gradients are principally an effect of biomass burning. These results show that detailed modeling using TM2 can provide good insight into the reasons for the observed latitudinal structure of $\delta^{13}CH_4$.

The simulation of $\delta^{13}CH_4$ values discussed here has been achieved without attempting to optimize the choice of source strengths or the spatial and temporal distribution of source types. Alternative choices of source strengths [e.g., *Francey et al.*, 1999] have been investigated which give a much better simulation of observed mixing ratios, but these underpredict the latitudinal gradients in $\delta^{13}CH_4$. This reflects the negative correlation that holds generally between mixing ratios and $\delta^{13}CH_4$ values. A more detailed analysis of the constraints on methane sources arising from the requirement to simulate both mixing ratios and $\delta^{13}CH_4$ and the role of the KIE in this will be presented separately. The important modeling result in this paper is that the unexpected observed latitudinal gradients in $\delta^{13}CH_4$ arise naturally from the model. We consider it relatively

unimportant for the present work that the magnitudes of latitudinal mixing ratio gradients are not exactly predicted.

An interesting property of the TM2 results is their day–to–day variability and the latitudinal change in that variability. Examples are shown in Figure 5. The top curve is from the grid cell centered on latitude 74.3°S and longitude 180°W. The seasonal cycle is fairly clean, with relatively small variability. In contrast, the bottom curve in Figure 5 from the grid cell centered on latitude 19.6°N and longitude 160°W has very large variability on short timescales and significant distortion of the underlying seasonal cycle in the latter part of the year. The model results are even more variable closer to the equator between the SPCZ and the ITCZ, consistent with the variability observed in the methane mixing ratios in this region.

The open triangles in Figure 3 show values of $\delta^{13}CH_4$ in the model grid cells that contain Scott Base, Baring Head, and the positions of the ship at the times indicated. The rapid variability described above and our employment of 1987 wind fields mean that a comparison on a timescale of 1 day between model results and observations is not useful. We have therefore provided "error bars" on the modeled values that represent the maximum and minimum $\delta^{13}CH_4$ obtained from the model within 10 days on either side of the ship measurement day. The error bars should give a rough estimate of year-to-year variability in the wind fields. The seasonal cycles at Scott Base and Baring Head are modeled reasonably, although the model cycle amplitudes are somewhat small and there is a small offset. The cycles determined from the ship transits at tropical latitudes are not well reproduced. This is understandable because of the large latitudinal gradients shown in Figure 3.
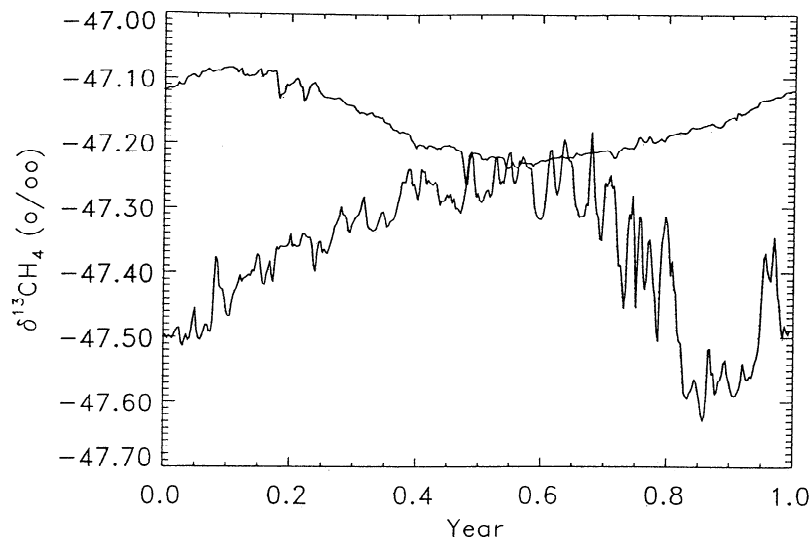
**Figure 5.** TM2 model time series of $\delta^{13}CH_4$ for the grid cell centered on latitude 74.3°S and longitude 180°W (top curve) and from the grid cell centered on latitude 19.6°N and longitude 160°W (bottom curve).

## 4. Conclusions

The shipboard data reported here show that the methane distribution in the Southern Hemisphere appears to be largely determined by interhemispheric transport with about a 5% difference in mixing ratio between the hemispheres and an abrupt gradient at the ITCZ. Significant variations in mixing ratio distributions between the ITCZ and the SPCZ were observed on the four voyages reported here, related to the intensity and position of the SPCZ. In June 1996, a well-defined SPCZ and ITCZ led to a confined region of well-mixed air around the equator, showing methane mixing ratios midway between the extratropical Southern and Northern Hemispheres. However, a relatively weak SPCZ in September 1997 led to uniform mixing ratios extending throughout the extratropical Southern Hemisphere and SPCZ to the ITCZ region. Complex tropical meteorology which results in changes in the intensity and position of the convergence zones clearly plays a major role in the distribution of atmospheric methane in tropical regions and its transport to the extratropical Southern Hemisphere.

Seasonal differences in the interhemispheric mixing ratio gradient were observed between the voyages, with the gradients observed on the November 1996 and September 1997 voyages about a factor of 2 greater than those observed in June 1996 and February 1997. The interhemispheric gradient for $\delta^{13}CH_4$ is also highly dependent on season, varying from a minimum of < 0.1‰ in June 1996 to a maximum of > 0.5‰ in November 1996. Lower values for $\delta^{13}CH_4$ were observed in the Northern Hemisphere north of the ITCZ. Interpolation of the data suggests that the average interhemispheric gradient in $\delta^{13}CH_4$ in the Pacific is 0.2-0.3‰, comparable to that predicted using the three-dimensional transport model TM2. The model simulates the main features of observed latitudinal and seasonal structure in surface values of $\delta^{13}CH_4$ quite well throughout the Pacific. However, it appears that good simulation of observed $\delta^{13}CH_4$ values is, to some extent, at the expense of good simulation of methane mixing ratios. The requirement that a methane source-sink budget be consistent with both types of data clearly imposes stricter constraints than arise from either mixing ratio or isotopic data alone.

The small gradients between the ITCZ and 35°S as well as the broad peak observed in $\delta^{13}CH_4$ in the southern tropics in September 1997 suggest that the seasonal cycles observed in the extratropical Southern Hemisphere are influenced by the southward transport of $^{13}C$ enriched methane from tropical biomass burning.

Analysis of the data shows that the seasonal cycles in $\delta^{13}CH_4$ fall into three distinct latitude bands differentiated by phase: (1) the extratropical Southern Hemisphere, (2) the extratropical Northern Hemisphere, and (3) tropical regions from ~15°S to 15°N encompassing the SPCZ and ITCZ. At 17°N, seasonal cycles in the tropics and the extratropical Northern Hemisphere with opposite phases result in the cancellation of the expected seasonal cycle in $\delta^{13}CH_4$.

The $\delta^{13}CH_4$ cycles in the extratropical Southern Hemisphere can be used to estimate a value for the apparent KIE of methane oxidation of 12-15‰, which is much larger than current laboratory measurements of the KIE of $CH_4$ + OH. The discrepancy can be explained by the competitive removal of methane by other chemistry, for example, active chlorine in the MBL. Using current published values for the KIEs and rate constants for $CH_4$ + OH and $CH_4$ +Cl, the $\delta^{13}CH_4$ data reported here suggest active chlorine levels of ~$10^4$ atoms .cm$^{-3}$ in the MBL. This is higher than most reported values but is consistent with recent model mechanisms describing routes to halogen activation predicting Cl concentrations in the MBL of 1-5 $10^4$ atoms .cm$^{-3}$ at steady state.

The data reported here demonstrate the value of simultaneous high-precision measurements of $\delta^{13}CH_4$ and methane mixing ratios as tools to probe latitudinal and seasonal structures in the Pacific region. However, far more high-precision $\delta^{13}CH_4$ data are needed to increase the scope of the method and to constrain 3-D chemical tracer models used to predict the global distribution of atmospheric methane.

# References

Bender, M.M., Variations in the $^{13}C/^{12}C$ ratios of plants in relation to the pathway of photosynthetic carbon dioxide fixation, *Phytochemistry, 10,* 1239-1244, 1971.

Bergamaschi, P., C.A.M. Brenninkmeijer, P.J. Crutzen, N.F. Elansky, I.B. Belikov, N.B.A. Trivett, and D.E.J. Worthy, Isotopic analysis based source identification for atmospheric $CH_4$ and CO sampled across Russia using the Trans-Siberian railroad, *J. Geophys. Res., 103,* 8227-8235, 1998.

Cantrell, C.A., R.E. Shetter, A.H. McDaniel, J.G. Calvert, J.A. Davidson, D.C. Lowe, S.C. Tyler, R.J. Cicerone, and J.P. Greenberg, Carbon kinetic isotope effect in the oxidation of methane by the hydroxyl radical, *J. Geophys. Res., 95,* 22,455-22,462, 1990.

Cicerone, R.J., and R.S. Oremland, Biogeochemical aspects of atmospheric methane, *Global Biogeochem. Cycles, 2,* 299-327, 1988.

Conny, J.M., and L.A. Currie, The isotopic characterization of methane, non-methane hydrocarbons and formaldehyde in the troposphere, *Atmos. Environ., 30,* 621-638, 1996.

DeMore, W.B., S.P. Sander, D.M. Goldan, R.F. Hampson, M.J. Kurylo, C.J. Howard, A.R. Ravishankara, C.E. Kolb, and M.J. Molina, Chemical kinetics and photochemical data for use in stratospheric modeling, *JPL Publ., 97-4,* 1997.

Denning, A.S., et al., Three-dimensional transport and concentration of $SF_6$: A model intercomparison study (TransCom 2), *Tellus,* in press, 1999.

Dlugokencky, E.J., L.P. Steele, P.M. Lang, and K.A. Masarie, The growth rate and distribution of atmospheric methane, *J. Geophys. Res., 99,* 17,021-17,043, 1994.

Etheridge, D.M., G.I. Pearman, and P.J. Fraser, Changes in tropospheric methane between 1841 and 1978 from a high accumulation-rate Antarctic ice core, *Tellus Ser. B, 44B,* 282-294, 1992.

Etheridge, D.M., L.P. Steele, R.J. Francey, and R.L. Langenfelds, Atmospheric methane between 1000 A.D. and present: Evidence of anthropogenic emissions and climatic variability, *J. Geophys. Res., 103,* 15,979-15,993, 1998.

Fishman, J., K. Fakhruzzaman, B. Cros, and D. Nganga, Identification of widespread pollution in the southern hemisphere deduced from satellite analysis, *Science, 252,* 1693-1696, 1991.

Francey, R.J., M.R. Manning, C.E. Allison, S.A. Coram, D.M. Etheridge, R.L. Langenfelds, D.C. Lowe, and L.P. Steele, A history of $\delta^{13}C$ in atmospheric $CH_4$ from the Cape Grim Air Archive and Antarctic firn air, *J. Geophys. Res.,* in press, 1999.

Fung, I., J. John, J. Lerner, E. Matthews, M. Prather, L.P. Steele, and P.J. Fraser, Three-dimensional model synthesis of the global methane cycle, *J. Geophys. Res. 96,* 13,033-13,065, 1991.

Gonfiantini, R., W. Stichler, and K. Rozanski, Standards and intercomparison materials distributed by the International Atomic Energy Agency for stable isotope measurements, in *Reference and Intercomparison Materials for Stable Isotopes of Light Elements,* edited by K. Rozanski, pp. 13-29, Int. Atomic Energy Agency, Vienna, 1993.

Graedel, T.E., and W.C. Keene, Tropospheric budget of reactive chlorine, *Global Biogeochem. Cycles, 9,* 47-77, 1995.

Greenberg, J.P., B. Lee, D. Helmig, and P.R. Zimmerman, Fully automated gas chromatographic-flame ionization detector system for the in situ determination of atmospheric non-methane hydrocarbons at low parts per trillion concentration, *J. Chromatogr., A676,* 389-398, 1994.

Gupta, M., S. Tyler, and R. Cicerone, Modeling atmospheric $\delta^{13}CH_4$ and the causes of recent changes in atmospheric $CH_4$ amounts, *J. Geophys. Res., 101,* 22,923-22,932, 1996.

Hao, W.M., and M.H. Liu, Spatial and temporal distribution of tropical biomass burning, *Global Biogeochem. Cycles, 8,* 495-503, 1994.

Hao, W.M., and D.E. Ward, Methane production from global biomass burning, *J. Geophys. Res., 98,* 20,657-20,661, 1993.

Heimann, M., The global atmospheric tracer model TM2, *Rep. 10,* Dtsch., Klimarechenzentrum, Hamburg, Germany, 1995.

Hein, R., P.J. Crutzen, and M. Heimann, An inverse modeling approach to investigate the global atmospheric methane cycle, *Global Biogeochem. Cycles, 11,* 43-76, 1997.

Houweling, S., F. Dentener, and J. Lelieveld, The impact of nonmethane hydrocarbon compounds on tropospheric chemistry, *J. Geophys. Res. 103,* 10,673-10,696, 1998.

Lang, P.M., L.P. Steele, and R.C. Martin, Atmospheric methane data for the period 1986-88 from the NOAA/CMDL global cooperative flask sampling network, *Rep. ERL CMDL-2,* Clim. Monit. and Diagnostics Lab., NOAA, Boulder, Colo., 1990.

Lang, P.M., L.P. Steele, L.S. Waterman, R.C. Martin, K.A. Masarie, and E.J. Dlugokencky, NOAA/CMDL Atmospheric methane data for the period 1983-1990 from shipboard flask samples, *Rep. ERL CMDL-4,* Clim. Monit. and Diagnostics Lab., NOAA, Boulder, Colo., 1992.

Lassey, K.R., D.C. Lowe, C.A.M. Brenninkmeijer, and A.J. Gomez, Atmospheric methane and its carbon isotopes in the southern hemisphere: Their time series and an instructive model, *Chemosphere, 26,* 95-109, 1993.

Lassey, K.R., D.C. Lowe, and M.R. Manning, The trend in atmospheric methane $\delta^{13}C$ and implications for isotopic constraints on the global methane budget, *Global Biogeochem. Cycles,* in press 1999.

Lowe, D.C., C.A.M. Brenninkmeijer, M.R. Manning, R.J. Sparks, and G.W. Wallace, Radiocarbon determination of atmospheric methane at Baring Head, New Zealand, *Nature, 372,* 522-525, 1988.

Lowe, D.C., C.A.M. Brenninkmeijer, S.C. Tyler, and E.J. Dlugokencky, Determination of the isotopic composition of atmospheric methane and its application in the Antarctic, *J. Geophys. Res., 96,* 15,455-15,467, 1991.

Lowe, D.C., C.A.M. Brenninkmeijer, G.W. Brailsford, K.R. Lassey, A.J. Gomez, and E.G. Nisbet, Concentration and $^{13}C$ records of atmospheric methane in New Zealand and Antarctica: Evidence for changes in methane sources, *J. Geophys. Res., 99,* 16,913-16,925, 1994.

Lowe, D.C., M.R. Manning, G.W. Brailsford, and A.M. Bromley, The 1991-1992 atmospheric methane anomaly: Southern hemisphere $^{13}C$ decrease and growth rate fluctuations, *Geophys. Res. Lett., 24,* 857-860, 1997.

Mak, J.E., and C.A.M. Brenninkmeijer, Compressed air sample technology for isotopic analysis of atmospheric carbon monoxide, *J. Atmos. Oceanic Technol., 11,* 425-431, 1994.

Prather, M., R. Derwent, D. Ehhalt, P. Fraser, E. Sanhueza, and X. Zhou, *Climate Change 1994: Radiative Forcing of Climate Change,* edited by J.T. Houghton, et al., pp. 73-126, Cambridge Univ. Press, New York, 1995.

Quay, P.D., S.L. King, J. Stutsman, D.O. Wilbur, L.P. Steele, I. Fung, R.H. Gammon, T.A. Brown, G.W. Farwell, P.M. Grootes, and F.H. Schmidt, Carbon isotopic composition of atmospheric $CH_4$: Fossil and biomass burning source strengths, *Global Biogeochem. Cycles, 5,* 25-47, 1991.

Salafsky, N., Drought in the rain forest: Effects of the 1991 El Nino-southern oscillation event on a rural economy in West Kalimantan, Indonesia, *Clim. Change, 27,* 373-396, 1994.

Sander, R., and P.J. Crutzen, Model study indicating halogen activation and ozone destruction in polluted air masses transported to the sea, *J. Geophys. Res., 101,* 9121-9138, 1996.

Saueressig, G., P. Bergamaschi, J.N. Crowley, H. Fischer, and G.W. Harris, Carbon kinetic isotope effect in the reaction of $CH_4$ with Cl atoms, *Geophys. Res. Lett., 22,* 1225-1228, 1995.

Saueressig, G., P. Bergamaschi, J.N. Crowley, C. Bruhl, and H. Fischer, Carbon and hydrogen kinetic isotope effects (KIE) of methane in its atmospheric chemical sink processes: New results for the reaction $CH_4$ + OH (abstract), *EGS Ann. Geophys.* in press, 1999.

Schimel, D., et al., Radiative forcing of climate change, in *Climate Change 1995: The science of Climate Change,* edited by J.T. Houghton, pp. 67-131, Cambridge Univ. Press, New York, 1996.

Singh, H.B., A.N. Thakur, and Y.E. Chen, Tetrachloroethylene as an indicator of low Cl atom concentrations in the troposphere, *Geophys. Res. Lett.*, *23*, 1529-1532, 1996.

Spivakovsky, C.M., R. Jevich, J.A. Logan, S.C. Wofsy, and M.B. McElroy, Tropospheric OH in a three-dimensional chemical tracer model: An assessment based on observations of $CH_3CCl_3$, *J. Geophys. Res.*, *95*, 18,441-18,471, 1990.

Stevens, C.M., and A. Engelkemeir, Stable carbon isotopic composition of methane from some natural and anthropogenic sources, *J. Geophys. Res.*, *93*, 725-733, 1988.

Stevens, C.S., and L. Krout, Method for the determination of the concentration and the carbon and oxygen isotopic composition of atmospheric carbon monoxide, *Int. J. Mass Spectrom. Ion Processes.*, *8*, 265-275, 1972.

Swinbanks, D., Forest fires cause pollution crisis in Asia, *Nature*, *389*, 321, 1997.

Trenberth, K.E., General characteristics of El Nino-southern oscillation, in *Teleconnections Linking Worldwide Climate Anomalies*, edited by M. Glantz, R.W. Katz, and N. Nicholls, pp. 13-41, Cambridge Univ. Press, New York, 1991.

Tyler, S.C., Kinetic isotope effects and their use in studying atmospheric trace species: Case study CH4 + OH, *Symp. Ser. 502*, pp. 390-408, Am. Chem. Soc., Washington, D.C., 1992.

Tyler, S.C., M. Keller, G. Brailsford, P. Crill, R. Stallard, and E. Dlugokencky, $^{13}C/^{12}C$ fractionation effect of microbial uptake on temperate forested and tropical seasonal soils (abstract), *Eos Trans. AGU*, *71*, 1260, 1990.

Tyler, S.C., P.M. Crill, and G.W. Brailsford, $^{13}C/^{12}C$ fractionation of methane during oxidation in a temperate forested soil, *Geochim. Cosmochim. Acta.*, *58*, 1629-1633, 1994.

Tyler, S.C., H.O. Ajie, A.L. Rice, R.J. Cicerone, and E.C. Tuazon, Experimentally determined kinetic isotope effects in the reaction of $CH_4$ with Cl: Implications for atmospheric $CH_4$ (abstract), *Eos Trans. AGU, 79*, (45), Fall Meet. Suppl., F102-103, 1998.

Tyler, S.C., H.O. Ajie, M.L. Gupta, R.J. Cicerone, D.R. Blake, and E.J. Dlugokencky, Stable Carbon isotopic composition of atmospheric methane: A comparison of surface level and free tropospheric air, *J. Geophys. Res.*, 104, 13, 895-13,910, 1999.

Vincent, D.G., The South Pacific convergence zone (SPCZ): A review, *Mon. Weather Rev.*, *122*, 1949-1970, 1994.

Vogt, R., P.J. Crutzen, and R. Sander, A mechanism for halogen release from sea-salt aerosol in the remote marine boundary layer, *Nature*, *383*, 327-330, 1996.

Wahlen, M., N. Tanaka, R. Henry, B. Deck, J. Zeglen, J.S. Vogel, J. Southon, A. Shemesh, A. Fairbanks, and W. Broecker, Carbon-14 in methane sources and in atmospheric methane: The contribution from fossil carbon, *Science, 245*, 286-290, 1989.

W. Allan, G. Brailsford, T. Bromley, D. Ferretti, A. Gomez, R. Knobben, D. C. Lowe, M. R. Manning, R. Martin, Z. Mei, and R. Moss, National Institute of Water and Atmospheric Research, 310 Evans Bay Parade, P.O. Box 14-901, Kilbirnie, Wellington, New Zealand. (d.lowe@niwa.cri.nz)

K. Koshy and M. Maata, School of Pure and Applied Sciences, University of the South Pacific, Suva, Fiji. (koshy_k@usp.ac.fj)